Journal of Fluids and Structures (1997) **11,** 351–366

INFLUENCE OF WALL THICKNESS ON RAYLEIGH CONDUCTIVITY AND FLOW-INDUCED APERTURE TONES

M. S. HOWE
Boston University, College of Engineering, 110 Cummington Street
Boston, MA 02215, U.S.A.

(Received 6 November 1996 and in revised form 17 January 1997)

A theoretical investigation is made of the effect of finite wall thickness on the interaction of a pressure perturbation, produced by sound or large-scale structural vibration, with a wall aperture in the presence of a tangential mean flow. Previous analyses for a wall of infinitesimal thickness (Howe, Scott & Sipcic) indicate that the perturbation is damped during the interaction if the Strouhal number based on aperture diameter and mean velocity is small. The damping is caused by the transfer of energy to the mean flow via the production of vorticity in the aperture. We show that the damping at low Strouhal numbers is unchanged when the wall has small, but finite, thickness, characteristic of real structures. However, wall thickness has a substantial influence on flow stability and on the excitation of self-sustained oscillations of fluid in the aperture. Instabilities exist when the Rayleigh conductivity, $K_R(\omega)$, of the aperture at frequency ω possesses poles in the upper ω-plane (an instability frequency being equal to the real part of ω at a pole); increasing wall thickness exacerbates the tendency towards instability by causing poles initially in the lower half plane to cross the real axis. Detailed results are given for two-sided flow which (for an ideal fluid) is stable for a wall of zero thickness when the flow speed is the same on both sides, and for one-sided flow over an aperture, which is unstable for arbitrary wall thickness. In both cases the instability frequencies are shown to progressively decrease as the wall thickness increases, but externally forced motion at low Strouhal numbers is always damped.

1. INTRODUCTION

NARROW BAND ACOUSTIC TONES are frequently generated by nominally steady, high Reynolds number flow over cavities and wall apertures (Rockwell 1983). The tones are associated with distinct ''operating stages'', each of which corresponds to a continuous range of Strouhal numbers governed by a *feedback* mechanism involving the periodic shedding of vorticity and its convection over the aperture or cavity opening (Rossiter 1962). Feedback occurs via impulsive pressures produced by the impingement of the vorticity on a downstream edge. The tonal amplitude varies with flow speed and exhibits abrupt, hysteretic jumps between stages. Empirical formulae for the different stages and their Strouhal number ranges are well known (Rossiter 1962; East 1966; Heller & Bliss 1975; Komerath *et al.* 1987; Ahuja & Mendoza 1995), although a general theory valid at arbitrary Mach number is still lacking (Tam & Block 1978; Bruggeman 1987; Bruggeman *et al.* 1989; Peters 1993; Hardin & Pope 1995; Kriesels *et al.* 1995).

A deductive theory of the resonance stages has been proposed by Howe (1997) for low Mach number, high Reynolds number flows, in situations where the wavelength of the generated sound is always large compared to the cavity or aperture diameter. This theory identifies the Strouhal numbers of the operating stages with the real parts of

0889–9746/97/040351 + 16 $25.00/fl970087

poles in the (upper) complex frequency plane of a certain impulse response function, which is equal to the Rayleigh conductivity for wall apertures and to an unsteady drag coefficient for shallow wall cavities. The response function is calculated on the basis of perturbation theory, in which the shear layer over the aperture or cavity is modelled by a *linearly* disturbed vortex sheet. Nonlinear factors must be invoked to limit the growth of instabilities predicted by this approach, but it is argued that finite amplitude motion of the shear layer does not significantly change the linear theory prediction of the resonance frequencies, which depend on the convection velocity, U_c, of disturbances within the shear layer. This hypothesis appears to be justified by experiments, which suggest that U_c is effectively independent of amplitude (Powell 1961; Holger *et al.* 1977; Blake & Powell 1986). Indeed, Howe (1977) obtains excellent agreement between predictions of this type of linear theory and published data for edge and cavity tones.

The analysis of Howe (1997) of the stability of flow over a rectangular aperture is applicable only for a wall of infinitesimal thickness, and was an extension of earlier, numerical studies for a circular aperture in a thin wall (Scott 1995; Howe, Scott & Sipcic 1996). In applications involving, say, sound waves incident on a perforated screen in the presence of mean flow, the wall thickness is not necessarily negligible compared to the aperture diameter. The zero-thickness approximation predicts that acoustic energy is always absorbed during such interactions (by transformation to the kinetic energy of vorticity generated at aperture edges) provided the Strouhal number based on aperture dimension and the mean flow speed is small. Vibrational energy can be absorbed by the same mechanism during tangential flow over a vibrating perforated plate (Maung & Howe 1997). In all such cases it is clearly desirable to incorporate the influence of finite wall thickness directly into the damping prediction scheme.

In this paper we do this for a rectangular aperture in a wall of small, but finite, thickness by generalizing the method of Howe (1997). Predictions are given for cases involving mean flow on one or both sides of the wall at a very high Reynolds number, when free shear layers may be modelled by vortex sheets. For an infinitely thin wall the flow is stable when the mean flow is the same on both sides [such that, for an ideal fluid, the mean vorticity vanishes in the steady state; see Howe *et al.* (1996)]; we demonstrate how this flow is destabilized by finite wall thickness by tracing the motions of poles of the Rayleigh conductivity from the lower to the upper halves of the complex frequency plane as wall thickness increases from zero. For one-sided flow (when the aperture is spanned by a plane vortex sheet in the undisturbed state), increasing wall thickness ultimately causes the Strouhal numbers of different instability stages to decrease to a common value, although the hypotheses of our thin wall approximation are strictly invalid when the wall thickness becomes comparable to the aperture diameter.

The analytical model for a wall of small, but finite, thickness is formulated in Section 2 for a rectangular aperture in the presence of an arbitrary, two-sided, low Mach number, high Reynolds number flow. Specific results are given in Sections 3 and 4, respectively, for two-sided uniform flow and one-sided flow.

2. THE GOVERNING EQUATIONS

2.1. The Rayleigh Conductivity

Consider high Reynolds number grazing flow at infinitesimal Mach number of fluid of uniform mean density, ρ_o, over both sides of a rectangular aperture in a plane, rigid wall of thickness d. The midplane of the wall is taken to coincide with the plane $x_2 = 0$ of the rectangular coordinate system (x_1, x_2, x_3), whose origin is at the geometrical center

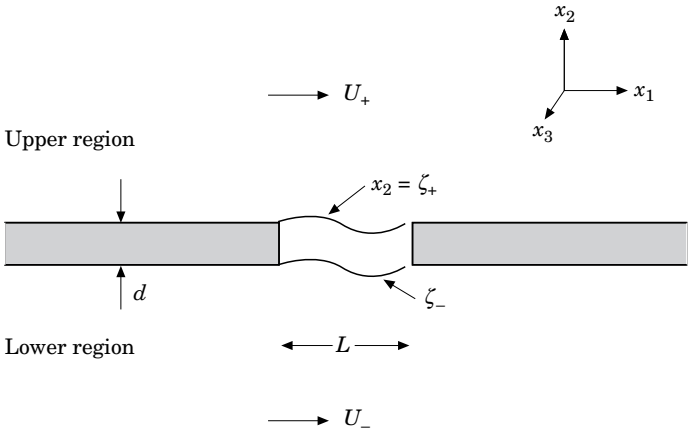

Figure 1. Idealized model of two-sided mean flow over a rectangular aperture in a wall of thickness d; the transverse length (out of the plane of the paper) of the aperture is b.

of the aperture. The mean flow is parallel to the x_1-axis with mean stream velocities U_+ and U_- in the "upper" and "lower" regions $x_2 \gtrless \pm\frac{1}{2}d$, respectively (see Figure 1). The aperture is aligned with sides of length L parallel to the mean flow and of length b in the transverse (x_3-) direction, so that the upper and lower openings occupy $|x_1| < s \equiv \frac{1}{2}L$, $x_2 = \pm\frac{1}{2}d$, $|x_3| < \frac{1}{2}b$. The shear layer over each opening is modelled by a vortex sheet, and the fluid within the volume of the aperture (in $|x_2| < \frac{1}{2}d$) is assumed to be in a mean state of rest.

Let uniform, small amplitude, time-dependent pressures, $p_\pm(t)$, be applied in the vicinity of the aperture, respectively in the upper and lower regions, and suppose the resulting motion of the vortex sheets is adequately described by linear perturbation theory. The motion produces a volume flux, $Q(t)$, through the aperture that is related to the applied pressure jump

$$[p_o(t)] \equiv p_+(t) - p_-(t)$$

by

$$\rho_o \, \partial \mathrm{Q(t)}/\partial t = -\int_{-\infty}^{\infty} K_R(\omega)[p_o(\omega)]\mathrm{e}^{-\mathrm{i}\omega t} \, \mathrm{d}\omega, \tag{2.1}$$

where $K_R(\omega)$ is the Rayleigh conductivity (Rayleigh 1945), which is a function of the radian frequency ω with the dimensions of length, and

$$[p_o(\omega)] \equiv (1/2\pi)\int_{-\infty}^{\infty} [p_o(t)]\mathrm{e}^{\mathrm{i}\omega t} \, \mathrm{d}t$$

is the Fourier transform of $[p_o(t)]$.

The instantaneous rate at which energy is dissipated at the aperture by the applied pressure field is $\Pi \equiv -Q(t)[p_o(t)]$, which is just the net rate of working of the applied pressure forces on the aperture. For time-harmonic fluctuations, where $[p_o(t)] \equiv \mathscr{R}e\{[p_o(\omega)]\mathrm{e}^{-\mathrm{i}\omega t}\}$, equation (2.1) enables Π to be expressed in the time-averaged form

$$\Pi(\omega) = -|[p_o]|^2 \, \mathscr{I}m\{K_R(\omega)\}/2\rho_o\omega \qquad (\omega > 0). \tag{2.2}$$

At high Reynolds number, when thermo-viscous losses are negligible, dissipation is the result of the direct transfer of energy from the applied pressure (an incident sound wave, say) to the kinetic energy of the mean flow. According to (2.2) this is the case

provided $\mathcal{I}m\{K_R(\omega)\} < 0$ (for $\omega > 0$). Negative damping occurs if $\mathcal{I}m\{K_R(\omega)\} > 0$, when energy is *extracted* from the mean flow. For a compressible fluid, Q represents the effective acoustic monopole source strength of the aperture, and a net gain in perturbation energy would be radiated as sound on either side of the wall.

These conclusions are applicable strictly for real values of the radian frequency ω. Equation (2.1) determines the volume flux resulting from the applied pressure differential $[p_o(t)]$, and a strictly causal evaluation of the integral demands that the path of integration from $\omega = \pm\infty$ should pass *above* all singularities of the integrand in the complex frequency plane. Since the applied pressure may be assumed to vanish prior to some finite time in the past, $[p_o(\omega)]$ is regular in $\mathcal{I}m\{\omega\} > 0$, and any singularities are associated with the conductivity $K_R(\omega)$. According to Howe (1997), these singularities are simple poles for one-sided mean flow (when $U_- \equiv 0$) over a rectangular aperture in a thin wall ($d = 0$); a comparison with experiment indicated that the real parts of the poles correspond to the various operating frequencies of self-sustained oscillations of the aperture shear layer. For uniform grazing flow ($U_+ \equiv U_-$), $K_R(\omega)$ is regular in $\mathcal{I}m(\omega) > 0$ for $d = 0$ (Howe *et al* 1996); in this case there is no vortex sheet across the aperture in the undisturbed state, and linear theory predicts that there are no self-sustained oscillations.

2.2. The Thin Wall Approximation

The equations of motion of the vortex sheets spanning the aperture openings of Figure 1 ($d \neq 0$) are similar to that discussed by Howe *et al.* (1996) for circular and rectangular apertures in a wall of infinitesimal thickness, and only a brief outline of the derivation is needed here.

Consider time-harmonic excitation of the aperture by a uniform pressure differential $[p_o(\omega)]\exp(-\mathrm{i}\omega t)$. Let $\zeta_\pm(x_1, x_3)\exp(-\mathrm{i}\omega t)$ respectively denote the displacement (in the x_2-direction) of the upper and lower vortex sheets from their undisturbed positions $x_2 = \pm\frac{1}{2}d$. At low Mach numbers the local motion may be regarded as incompressible, and linearized representations of the perturbation pressures above and below the wall have the forms

$$\left.\begin{aligned} p &= p_+ - \rho_o\left(\omega + \mathrm{i}U_+\frac{\partial}{\partial x_1}\right)^2 \int_s \frac{\zeta_+(y_1, y_3)}{2\pi\,|\mathbf{x}-\mathbf{y}|}\,\mathrm{d}y_1\,\mathrm{d}y_3, \qquad x_2 > \tfrac{1}{2}d \\ &= p_- + \rho_o\left(\omega + \mathrm{i}U_-\frac{\partial}{\partial x_1}\right)^2 \int_s \frac{\zeta_-(y_1, y_3)}{2\pi\,|\mathbf{x}-\mathbf{y}|}\,\mathrm{d}y_1\,\mathrm{d}y_3, \qquad x_2 < -\tfrac{1}{2}d, \end{aligned}\right\} \tag{2.3}$$

where respectively $\mathbf{y} = (y_1, \pm\frac{1}{2}d, y_3)$, the integration is over the aperture cross-section S, and the exponential time factor $\exp(-\mathrm{i}\omega t)$ is here and hereinafter suppressed. Note that, according to linear theory, vorticity impinging on the downstream edge of the aperture remains in the plane of the (upper or lower) surface of the wall, where its subsequent influence on the unsteady flow is annulled by image vorticity in the wall.

In the thin wall approximation the wavelength of motions of the vortex sheets is assumed to be large compared to the wall thickness d. In these circumstances the fluid displacement ζ in the x_2-direction within the aperture may be assumed to be independent of x_2, i.e., we can take

$$\zeta \equiv \zeta(x_1, x_3) = \zeta_+(x_1, x_3) = \zeta_-(x_1, x_3). \tag{2.4}$$

Then the equation of motion of a "column" of fluid within the aperture is just

$$\rho_o d\,\partial^2\zeta/\partial t^2 = -[p], \qquad |x_1| < s, \qquad |x_3| < \tfrac{1}{2}b,$$

where $[p]$ is the difference in the pressures applied to the upper and lower ends of the column at $x_2 = \pm\frac{1}{2}d$. For time-harmonic motion, equations (2.3) accordingly imply that

$$\left[\left(\omega + \mathrm{i}U_+\frac{\partial}{\partial x_1}\right)^2 + \left(\omega + \mathrm{i}U_-\frac{\partial}{\partial x_1}\right)^2\right]\frac{1}{2\pi}\int_s \frac{\zeta(y_1, y_3)\,\mathrm{d}y_1\,\mathrm{d}y_3}{\sqrt{(x_1 - y_1)^2 + (x_3 - y_3)^2}} + d\omega^2\zeta(x_1, x_3) = \frac{[p_o]}{\rho_o}. \tag{2.5}$$

This equation is simplified by means of the hypothesis that vortex shedding from the straight end $x_1 = -s$ of the aperture produces strongly correlated motions of the vortex sheets at different transverse locations x_3, so that ζ may be assumed to be independent of x_3. Equation (2.5) may then be explicitly integrated over the transverse span of the aperture with respect to both y_3 and x_3, and the result cast in the form

$$\left[\left(\sigma + \mathrm{i}\frac{\partial}{\partial\xi}\right)^2 + \left(\sigma + \mathrm{i}\mu\frac{\partial}{\partial\xi}\right)^2\right]\int_{-1}^{1}\zeta(\eta)\{\ln|\xi - \eta| + \mathscr{L}(\xi, \eta)\}\,\mathrm{d}\eta$$
$$- 2\pi\left(\frac{d}{L}\right)\sigma^2\zeta(\xi) = -\pi s[p_o]/\rho_o U_+^2, \qquad |\xi| < 1, \tag{2.6}$$

where

$$\left.\begin{aligned} \sigma = \omega s/U_+, \qquad \mu = U_-/U_+, \qquad \xi = x_1/s, \qquad \eta = y_1/s, \\ \mathscr{L}(\xi, \eta) = -\ln\{b/s + \sqrt{[(b/s)^2 + (\xi - \eta)^2]}\} + \sqrt{[1 + (s/b)^2(\xi - \eta)^2]} - (s/b)\,|\xi - \eta|. \end{aligned}\right\} \tag{2.7}$$

Equation (2.6) is next integrated with respect to the second order differential operator on the left-hand side by introducing the Green's function

$$G(\xi, \eta) = \frac{1}{2\sigma(1 - \mu)}(H(\xi - \eta)\mathrm{e}^{\mathrm{i}\sigma_+(\xi - \eta)} + H(\eta - \xi)\mathrm{e}^{\mathrm{i}\sigma_-(\xi - \eta)}), \tag{2.8}$$

which is a particular solution of

$$\left[\left(\sigma + \mathrm{i}\frac{\partial}{\partial\xi}\right)^2 + \left(\sigma + \mathrm{i}\mu\frac{\partial}{\partial\xi}\right)^2\right]G(\xi, \eta) = \delta(\xi - \eta).$$

In these formulae, $H(x)$ is the Heaviside unit function ($=0, 1$ accordingly as $x \lessgtr 0$), and $\sigma_\pm$ are the Kelvin–Helmholtz wavenumbers (Lamb 1932)

$$\sigma_\pm = \sigma\left(\frac{1 \pm \mathrm{i}}{1 \pm \mathrm{i}\mu}\right). \tag{2.9}$$

The dimensionless displacement

$$Z(\xi) \equiv \frac{-2\rho_o\omega^2 s}{\pi[p_o]}\zeta(\xi), \tag{2.10}$$

then satisfies the following integrated form of equation (2.6)

$$\int_{-1}^{1} Z(\eta)\{\ln|\xi - \eta| + \mathscr{L}(\xi, \eta)\}\,\mathrm{d}\eta - 2\pi\sigma^2(d/L)\int_{-1}^{1} Z(\eta)G(\xi, \eta)\,\mathrm{d}\eta$$
$$+ \lambda_+\mathrm{e}^{\mathrm{i}\sigma_+\xi} + \lambda_-\mathrm{e}^{\mathrm{i}\sigma_-\xi} = 1, \qquad |\xi| < 1, \tag{2.11}$$

where $\lambda_\pm$ are constants of integration.

The integral equation (2.11) is readily solved by collocation, by the procedure described by Scott (1995) for a vortex sheet over a circular aperture. The values of $\lambda_\pm$ are fixed by imposing the Kutta condition that the vortex sheets should leave the upstream edges of the aperture smoothly, i.e., by requiring that $\zeta = \partial\zeta/\partial\xi = 0$ as $\xi \to -1$ (Crighton 1985). No further conditions can be imposed at the trailing edge ($\xi = 1$), where the displacement must be permitted to develop a mild, yet integrable potential flow singularity. This singularity is the linear theory representation of the large amplitude edge motion observed in experiments.

The aperture volume flux $Q(\omega) = -\mathrm{i}\omega b \int_{-s}^{s} \zeta(x_1)\,\mathrm{d}x_1$, from which relation it is readily deduced that the Rayleigh conductivity is given in terms of Z by

$$K_R = -\frac{1}{2}\pi b \int_{-1}^{1} Z(\eta)\,\mathrm{d}\eta. \tag{2.12}$$

The conductivity is generally a complex valued function of the frequency ω, but also depends on the aperture aspect ratio b/L, the wall thickness ratio d/L, and the mean velocity ratio $\mu = U_-/U_+$.

In the special case of uniform, two-sided mean flow, where $U_- = U_+ \equiv U$, the wavenumbers σ_+ and σ_- are both equal to $\sigma = \omega s/U$, and it is convenient to take Green's function (2.8) in the degenerate form

$$G(\xi, \eta) = -H(\xi - \eta)(\xi - \eta)\mathrm{e}^{\mathrm{i}\sigma(\xi-\eta)}.$$

The terms in $\lambda_\pm$ in equation (2.11) should then be replaced by $(\lambda_1 + \lambda_2\xi)\mathrm{e}^{\mathrm{i}\sigma\xi}$, where λ_1, λ_2 are constants determined by the Kutta condition.

3. UNIFORM, TWO-SIDED FLOW OVER A RECTANGULAR APERTURE

Equations (2.11) and (2.12) are first applied to investigate the stability of nominally steady flow over an aperture in a uniform grazing mean flow, where $U_- = U_+ \equiv U$ (Figure 2). Linear theory predicts this flow to be stable when $d = 0$.

3.1. Dependence of Rayleigh Conductivity on Wall Thickness

Representative plots are shown in Figure 3 of the real and imaginary parts of the dimensionless conductivity

$$K_R(\omega)/b = \Gamma_R(\omega) - \mathrm{i}\Delta_R(\omega), \tag{3.1}$$

for real values of $\sigma = \omega s/U$, when the aspect ratio $b/L = 2$ and for a range of values of $d/L < 1$. These results are typical of all aspect ratios. K_R has been calculated from the numerical solution of equation (2.11), modified as described in the last paragraph of Section 2. According to (2.2), perturbation energy is dissipated at the aperture at those frequencies where $\Delta_R(\omega) > 0$. Figure 3 shows that Δ_R is positive and effectively

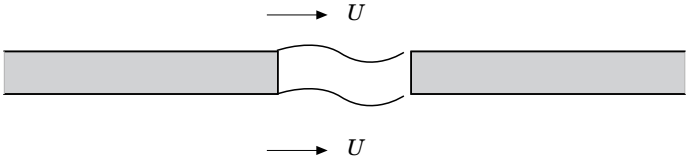

Figure 2. Uniform grazing mean flow over a rectangular aperture.

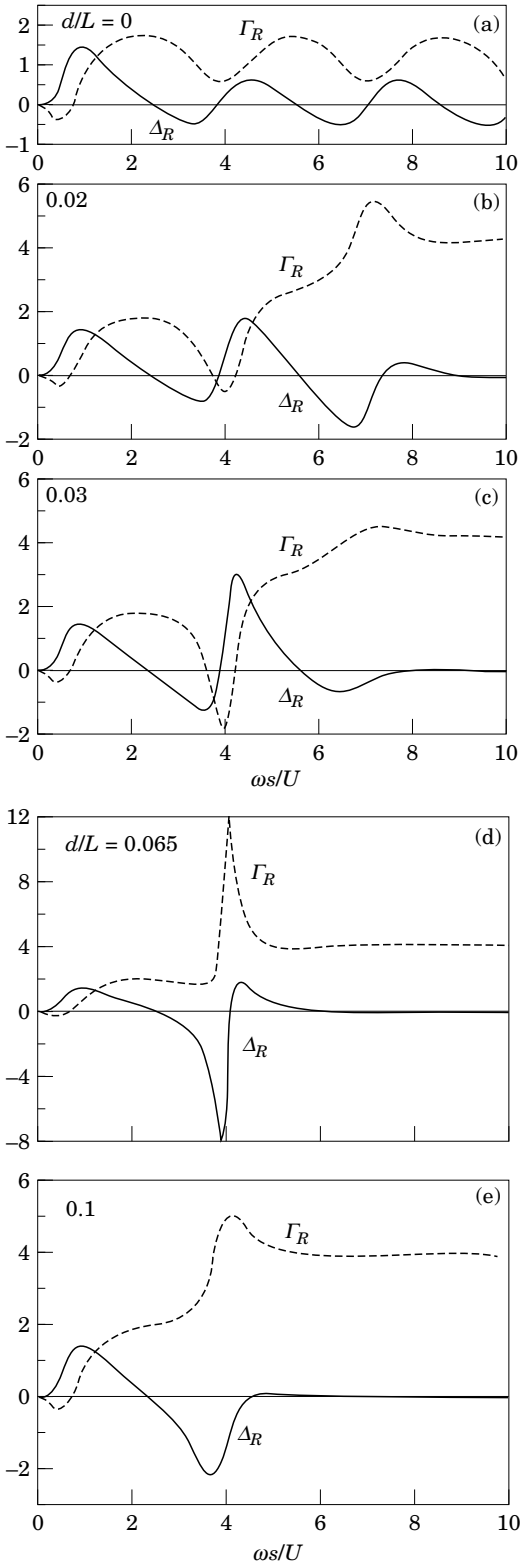

Figure 3. Illustrating the dependence of $K_R(\omega)/b = \Gamma_R(\omega) - i\Delta_R(\omega)$ on frequency when $U_- = U_+ \equiv U$ for $b/L = 2$ and for (a) $d/L = 0$, (b) $d/L = 0{\cdot}02$, (c) $d/L = 0{\cdot}03$, (d) $d/L = 0{\cdot}065$, (e) $d/L = 0{\cdot}1$, (f) $d/L = 0{\cdot}2$, (g) $d/L = 0{\cdot}5$.

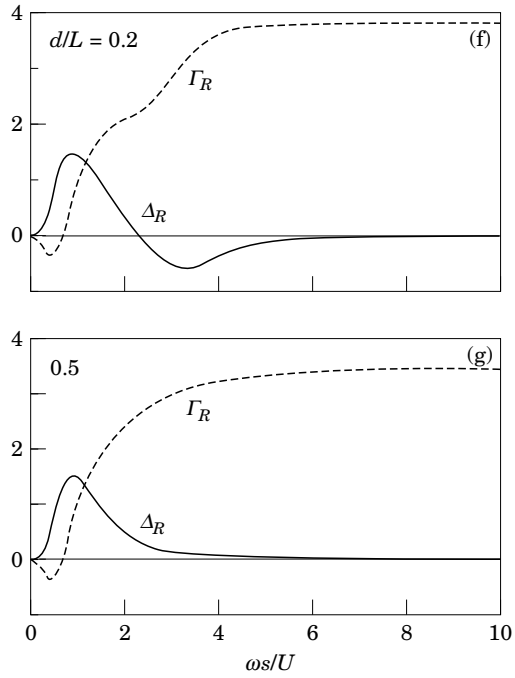

Figure 3. *Continued*.

invariant with changing d/L in the low frequency region $\omega s/U < 2{\cdot}4$, where energy is always dissipated. This conclusion is important because it suggests that the effectiveness of perforated, grazing flow screens used to absorb low Strouhal number sound and vibration is not significantly dependent on screen thickness.

According to Figure 3(a), $K_R(\omega)$ varies periodically when $\omega s/U > 2$ and $d/L = 0$. However, the influence of small, but finite, wall thickness is always felt at sufficiently high frequencies, when the second integral on the left of (2.11), which represents the inertia of fluid in the aperture, becomes important. This causes the oscillations in the real and imaginary parts of $K_R(\omega)$ ultimately to die out as σ becomes large. We shall demonstrate below that the aperture motion is absolutely unstable when $d/L \neq 0$; indeed, when d/L exceeds about 0·1 [Figure 3(e)] $\Gamma_R(\omega)$ and $\Delta_R(\omega)$ vary with frequency in qualitatively the same way as for an aperture in the presence of an unstable, one-sided mean flow (Howe *et al.* 1996; see also Section 4). In Figure 3(g) ($d/L = 0{\cdot}5$) the imaginary component $\Delta_R > 0$ for all $\omega > 0$, which implies that forced motion at the real frequency ω is always damped; this conclusion should be treated with caution, however, since the present thin wall theory may not be strictly valid for such a large value of d/L.

3.2. Poles of the Conductivity

An understanding of the changes in $\Gamma_R(\omega)$ and $\Delta_R(\omega)$ with increasing values of d/L can be obtained from the asymptotic approximation given by Howe *et al.* (1996, Section 3) for $d/L = 0$ and $b/L \gg 1$, namely

$$K_R \approx \frac{\pi b}{2\{F(\sigma) + \ln(8b/\mathrm{e}L)\}}, \tag{3.2}$$

where $e \approx 2{\cdot}718$ is the exponential constant, and

$$F(\sigma) = \frac{i\sigma J_0(J_0 - iJ_1) - [J_0 - 2i\sigma(J_0 - iJ_1)][J_0 - i\sigma(J_0 + iJ_1)]}{\sigma[J_0 J_1 + \sigma\{J_1^2 + (J_0 - 2iJ_1)^2\}]}, \tag{3.3}$$

$J_{0,1} \equiv J_{0,1}(\sigma)$ being Bessel functions. The variations with σ of Γ_R and Δ_R predicted by this formula are similar to those shown in Figure 3(a) ($d/L = 0$) for $b/L = 2$, becoming periodic when σ exceeds about 2, where

$$F \approx -2/\{1 - ie^{-2i\sigma}\},$$

so that $K_R(\omega)$ has simple poles at

$$\sigma \equiv \frac{\omega s}{U} \approx (n + \tfrac{1}{4})\pi + \frac{i}{2}\ln\left(\frac{1}{2} - \frac{1}{\ln\{8b/eL\}}\right), \qquad n = 1, 2, \ldots \tag{3.4}$$

These poles lie in the lower half, $\mathcal{I}m(\omega) < 0$, of the frequency plane provided $b/L > e^3/8 \approx 2{\cdot}51$, which is always satisfied when the asymptotic formula (3.2) is applicable. Numerical computation indicates the presence of an additional pole, not given by this formula, on the negative imaginary axis.

The asymptotic formula (3.2) supplies a qualitative picture of the behavior of $K_R(\omega)$ also for $b/L = 2$ and $d/L = 0$ [the case considered in Figure 3(a)]; the motion is stable and poles of K_R are all in the lower frequency plane. The real parts of these poles are close to those defined by (3.4), and correspond approximately to the locations of successive *minima* of $\Gamma_R(\omega)$ in Figure 3(a) near $\omega s/U = 3{\cdot}9$, $7{\cdot}1$, $10{\cdot}2$, etc. An indication of what happens to these poles as d/L increases from zero can be surmised from Figure 3.

Consider, in particular, the pole whose real part is near $\sigma_o = 3{\cdot}9$ at $d/L = 0$. The rapid variations near this frequency exhibited by $\Gamma_R(\omega)$ and $\Delta_R(\omega)$ in Figures 3(c) and 3(d) imply that the pole is close to the real axis for $0{\cdot}03 < d/L < 0{\cdot}065$. If the location of the pole is approximated by

$$\sigma \equiv \sigma_o + i\epsilon,$$

where ε is real, then the curves in Figure 3(c) are consistent with a local variation in the neighborhood of $\sigma = \sigma_o$ defined by

$$\Gamma_R - i\Delta_R \approx \text{constant} - \frac{i\alpha}{\sigma - \sigma_o - i\epsilon}, \qquad \text{where } \alpha > 0,$$

i.e.

$$\Gamma_R \approx \text{constant} + \frac{\alpha\epsilon}{(\sigma - \sigma_o)^2 + \epsilon^2}, \qquad \Delta_R \approx \frac{\alpha(\sigma - \sigma_o)}{(\sigma - \sigma_o)^2 + \epsilon^2}.$$

When $\alpha > 0$ and ϵ is small and *negative* (the pole being just below the real axis), Γ_R exhibits a deep negative minimum at $\sigma \equiv \omega s/U = \sigma_0$, as in Figure 3(c) near $\sigma = 3{\cdot}9$. When d/L increases to $0{\cdot}065$, Figure 3(d) shows that the negative minimum has been transformed into a sharp maximum. Since the inflexional behaviour of Δ_R is the same in each of these cases, this change must have occurred because of a reversal in the sign of ϵ, i.e., because the pole has crossed the real axis into the upper half-plane.

The Newton–Raphson procedure and numerical predictions of $1/K_R(\omega)$ supplied by (2.12) can be used to track the motion of poles into the upper half-plane as d/L increases from zero, by starting from initial trial values given by (3.4) for a given value of n. Poles in the upper frequency plane correspond to spontaneously excited

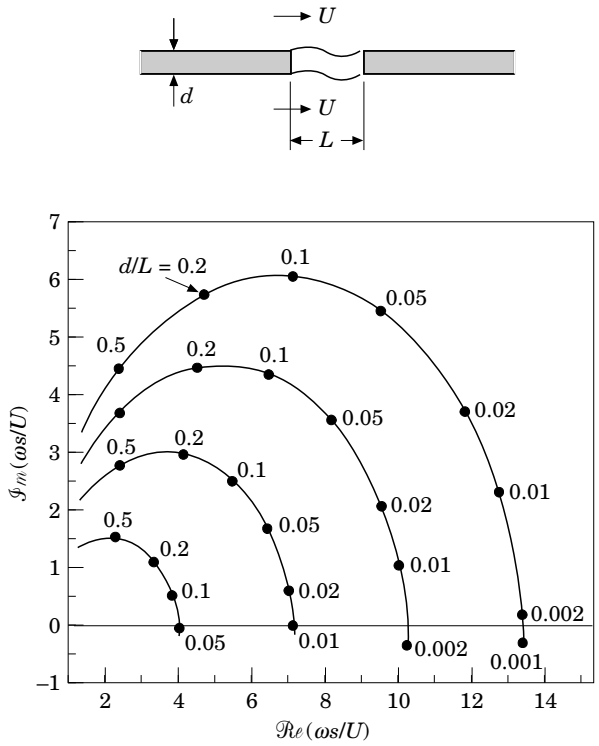

Figure 4. Loci of poles of $K_R(\omega)$ in the complex frequency plane for $U_+ = U_- \equiv U$ for the first four operating stages $n = 1 - 4$ when $b/L = 2$.

instabilities. Figure 4 illustrates pole loci for the first four "operating stages", $n = 1 - 4$, when the aspect ratio $b/L = 2$, and reveals that high frequency, high order instabilities (n large) are the first to be excited as d/L becomes finite. All instability modes are possible when d/L exceeds about 0·05. When d/L *decreases* from this value, the poles corresponding to $n = 1, 2, 3,$ etc, successively cross into the lower half-plane; the first four stages are stable when d/L is less than about 10^{-3}. This figure also shows that the various poles converge onto the imaginary axis when d/L becomes large, and that their real parts become approximately equal, although the present thin wall approximation is probably not applicable for $d/L \geq 0{\cdot}5$. The results are presented differently in Figure 5, where the dependence of the Strouhal number fL/U on d/L (where $f = \mathscr{R}e(\omega)/2\pi$ for the pole at ω) is shown for the first four operating stages. Each curve starts on the left at that finite, non-zero value of d/L at which the corresponding pole crosses into the upper frequency plane.

These predictions are for $b/L = 2$. However, similar results are obtained for arbitrary values of the aspect ratio b/L. This is illustrated by the example of Figure 6, which gives the Strouhal number dependence on d/L for $b/L = 500$, i.e., for an aperture in the form of a long, transverse slot.

4. ONE-SIDED FLOW OVER A RECTANGULAR APERTURE

4.1. Instability of One-sided Flow

Let the mean flow be confined to the upper region of Figure 1 (i.e., $U_- \equiv 0$). In the steady state a vortex sheet separates the uniform flow at speed $U_+ \equiv U$ from the stagnant fluid within and below the aperture. The sheet is unstable for arbitrary wall

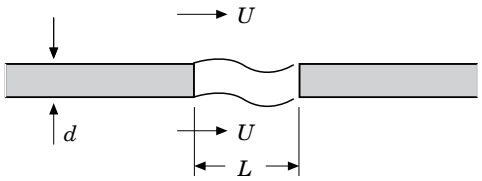

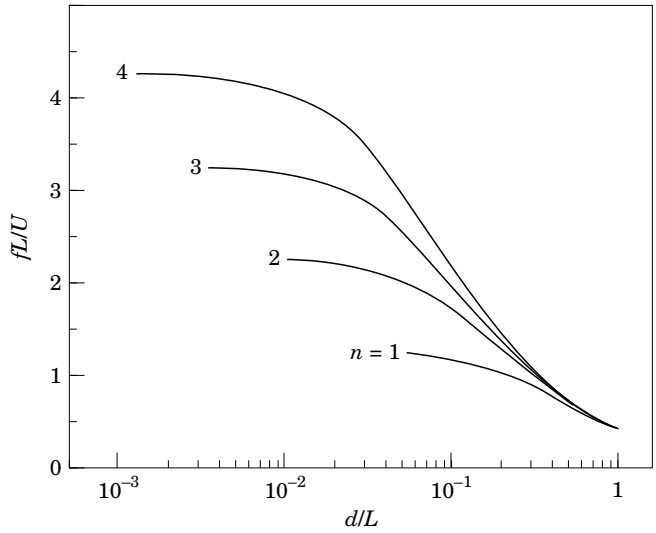

Figure 5. Strouhal number dependence on wall thickness for two-sided uniform flow ($U_+ = U_- \equiv U$) when $b/L = 2$.

thickness, and $K_R(\omega)$ must therefore have poles in the upper frequency plane. This may be contrasted with the uniform, two-sided flow of Section 3, which is stable when $d = 0$. However, two-sided flow is also unstable for $d = 0$ when the aperture supports a mean shear ($U_+ \neq U_-$). The manner in which this instability arises can be illustrated in terms of the analytical approximation (3.2) for $K_R(\omega)$ for $b/L \gg 1$; when $U_+ \neq U_-$, the definition (3.3) is replaced by (Howe *et al.* 1996)

$$F(\sigma) = \frac{-\sigma_+ J_0(\sigma_-)[J_0(\sigma_+) - 2W(\sigma_+)] + \sigma_- J_0(\sigma_+)[J_0(\sigma_-) - 2W(\sigma_-)]}{\sigma_+ W(\sigma_-)[J_0(\sigma_+) - 2W(\sigma_+)] - \sigma_- W(\sigma_+)[J_0(\sigma_-) - 2W(\sigma_-)]}, \tag{4.1}$$

where $W(x) = \mathrm{i}x[J_0(x) - \mathrm{i}J_1(x)]$ and $\sigma_\pm$ are defined as in (2.9).

This formula can be used to calculate the loci of the poles from their initial locations in $\mathcal{I}m(\omega) < 0$, given by (3.4), as $\mu \equiv U_-/U_+$ decreases from 1 to 0. The result is depicted in Figure 7 for the first four operating stages. As for the case of destabilization by increasing wall thickness (Section 3.2), higher order poles are the first to cross into the upper half plane as U_-/U_+ decreases; all of the poles lie in $\mathcal{I}m(\omega) > 0$ when $U_-/U_+ < 0{\cdot}47$. These plots are for the quasi-two-dimensional aspect ratio $b/L = 500$, but are typical of the behavior for arbitrary values of b/L. Ultimately, when $U_- = 0$, the poles for large values of n lie along a ray making an angle of 45° with the positive real axis (a related set of poles, corresponding to $n < 0$ in (3.4) lies asymptotically along the image of this ray in the imaginary axis). According to (3.4), when $U_-/U_+ = 1$ the real parts of successive poles differ by about π. As U_-/U_+ decreases, this difference gradually diminishes, until when $U_- = 0$ both their real *and* imaginary parts differ by

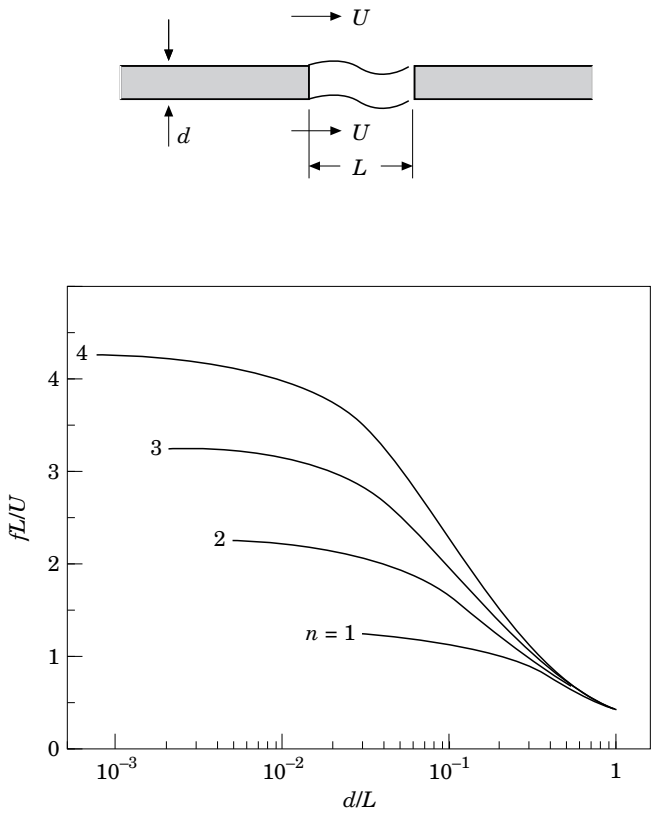

Figure 6. Strouhal number dependence on wall thickness for two-sided uniform flow ($U_+ = U_- \equiv U$) when $b/L = 500$.

about $\frac{1}{2}\pi$. This means that the jump in Strouhal number fL/U between successive stages of the aperture tones is about $\frac{1}{2}$ when $d = 0$ (Howe 1997).

4.2. Conductivity for Finite Wall Thickness

The conductivity $K_R(\omega)$ for one-sided flow and real ω is calculated from equations (2.11) and (2.12), and does not vary significantly with d/L except when d/L is greater than about 0·2. This is illustrated in Figure 8 for an aspect ratio $b/L = 2$. The real part, $\Gamma_R(\omega)$, hardly changes at all with increasing d/L and, as in the case of two-sided uniform flow, $\Delta_R(\omega) > 0$ when $\omega s/U$ is small (less than about 1·5), at which frequencies forced motion of the shear layer by the applied pressure load $[p_o]$ is always damped; the variation of $\Delta_R(\omega)$ with ω is effectively independent of d/L in this frequency range. For larger values of $\omega s/U$ energy is extracted from the flow and supplied to the perturbing field where $\Delta_R(\omega) < 0$.

In Figure 3, for two-sided uniform flow, the rapid changes in the form of $K_R(\omega)$ with varying d/L are produced by poles crossing the real axis. In the present case the poles are already in the upper half-plane when $U_- = 0$ and $d = 0$, and their subsequent motions when d/L increases from zero causes relatively minor changes in $K_R(\omega)$. These motions (from initial positions indicated in Figure 7 at $U_-/U_+ = 0$) are plotted in Figure 9 for the first four operating stages when $b/L = 500$. $\mathcal{R}e(\omega s/U)$ becomes approximately the same for the poles shown in the figure when d/L is larger than

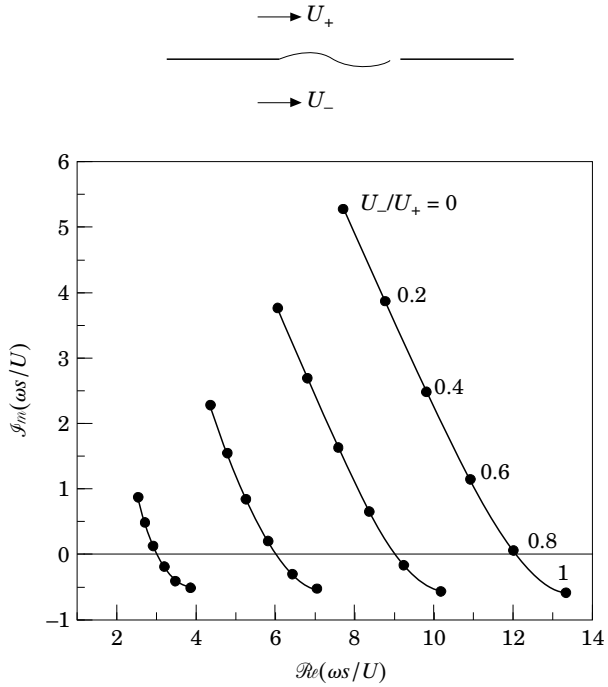

Figure 7. Loci of poles of $K_R(\omega)$ in the complex frequency plane for $d/L = 0$, $b/L = 500$ and $0 \leq U_-/U_+ \leq 1$ for the first four operating stages $n = 1 - 4$.

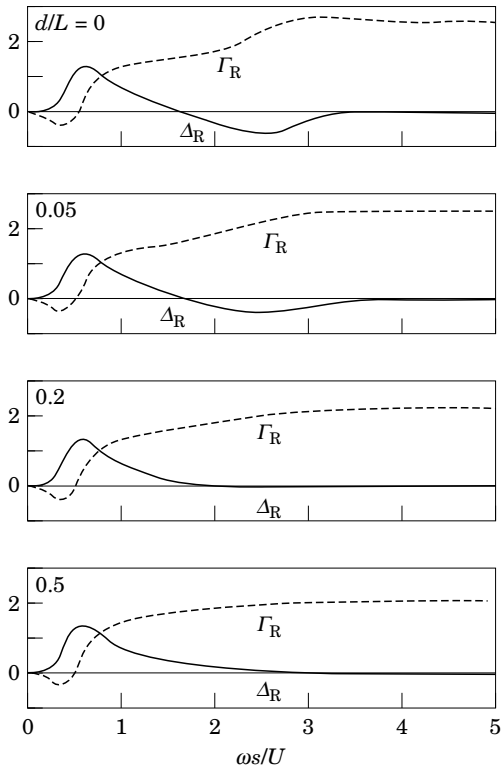

Figure 8. The dependence of $K_R(\omega)/b = \Gamma_R(\omega) - i\Delta_R(\omega)$ on frequency when $U_- = 0$ for $b/L = 2$ and for $d/L = 0$, 0·05, 0·2, 0·5.

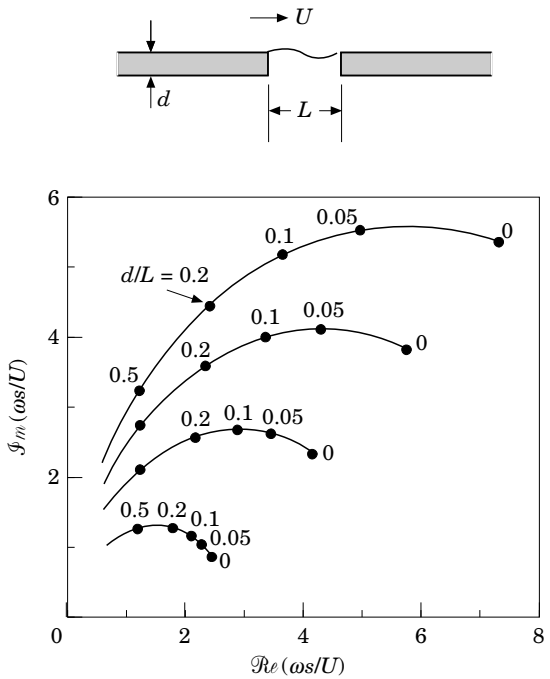

Figure 9. Loci of poles of $K_R(\omega)$ in the complex frequency plane for $U_- = 0$ for the first four operating stages $n = 1 - 4$ when $b/L = 500$.

about 0·4, i.e. the Strouhal numbers of the operating stages become equal. One-sided flow is unstable for all values of d/L; Figure 10 shows how the Strouhal numbers $fL/U = \mathscr{R}e(\omega s/\pi U)$ change with d/L for $b/L = 500$. Results for smaller aspect ratios are qualitatively and quantitatively similar, and will not be given here.

5. CONCLUSION

Vortex shedding in wall apertures in the presence of grazing mean flow is responsible for an exchange of energy between the mean flow and an applied pressure, associated, for example, with a sound wave incident on the wall or with pressures generated by structural vibrations. Previous analytical treatments of such interactions for an infinitely thin wall have predicted that the applied perturbation is damped (energy being transferred to the mean flow) provided the Strouhal number is sufficiently small. In this paper the magnitude of this low Strouhal number damping has been shown to be effectively unchanged when the wall has small, but finite, thickness, characteristic of real structures.

In all cases, however, finite thickness *does* modify the stability of the motion. For high Reynolds number two-sided flow, when the mean velocity is the same on both sides, the aperture flow is linearly stable for a wall of zero thickness. The mean shear layers introduced by finite wall thickness destabilize the flow, mathematically because increasing thickness is responsible for the migration of poles of the Rayleigh conductivity into the upper half of the complex frequency plane. The instabilities are here interpreted as tonal, self-sustained oscillations of the flow, whose frequencies occur in discrete bands (or "stages") as the wall thickness varies, at values equal to the real parts of the instability poles. The absence of experimental data for aperture flows

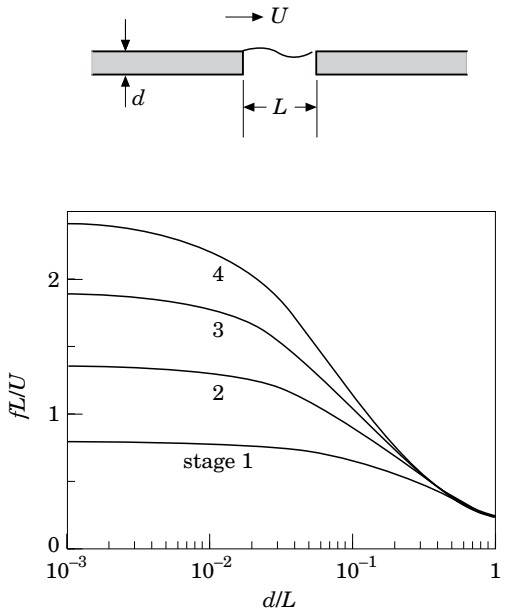

Figure 10. Strouhal number dependence on wall thickness for one-sided flow ($U_- = 0$) when $b/L = 500$ for the first four operating stages.

of this type precludes a direct experimental validation of this hypothesis. However, Howe (1997) has reported excellent agreement with published data for frequency predictions of the same theory applied to edge-tones and shallow wall-cavity tones. The amplitudes of the oscillations are controlled by nonlinear mechanisms not discussed in this paper, and are typically independent of the presence of any other applied pressure perturbation.

One-sided flow over an aperture is unstable for arbitrary wall thickness. As the wall thickness increases from zero, for either one or two-sided flow, the frequencies of the instability modes progressively decrease, and ultimately approach a common value, although it is uncertain whether the approximation of this paper remains valid in this limit. At low Strouhal numbers, forced motion of an aperture by an applied pressure is always damped.

ACKNOWLEDGEMENT

This work was sponsored by the Air Force Office of Scientific Research under Grant No. F49620-96-1-0098, administered by Major Brian Sanders.

References

Ahuja, K. K. & Mendoza, J. 1995 Effects of cavity dimensions, boundary layer, and temperature on cavity noise with emphasis on benchmark data to validate computational aeroacoustic codes. NASA Contractor Report: Final Report Contract NAS1–19061, Task 13.

Blake, W. K. & Powell, A. 1986 The development of contemporary views of flow-tone generation. In *Recent Advances in Aeroacoustics* (eds A. Krothapali & C. A. Smith), pp. 247–325. New York: Springer.

Bruggeman, J. C. 1987 Flow induced pulsations in pipe systems. Ph.D. Thesis, Eindhoven University of Technology, Eindhoven, The Netherlands.

Bruggeman, J. C., Hirschberg, A., van Dongen, M. E. H., Wijnands, A. P. J. & Gorter,

J. 1989 Flow induced pulsations in gas transport systems: anslysis of the influence of closed side branches. *ASME Journal of Fluids Engineering* **111,** 484–491.

CRIGHTON, D. G. 1985 The Kutta condition in unsteady flow. *Annual Review of Fluid Mechanics* **17,** 411–445.

EAST, L. F. 1966 Aerodynamically induced resonance in rectangular cavities. *Journal of Sound and Vibration* **3,** 277–287.

HARDIN, J. C. & POPE, D. S. 1995 Sound generation by flow over a two-dimensional cavity. *American Institute of Aeronautics and Astronautics Journal* **33,** 407–412.

HELLER, H. H. & BLISS, D. B. 1975 The physical mechanism of flow-induced pressure fluctuations in cavities and concepts for their suppression. American Institute of Aeronautics and Astronatutics Paper 75–491.

HOLGER, D. K., WILSON, T. A. & BEAVERS, G. S. 1977 Fluid mechanics of the edgetone. *Journal of the Acoustical Society of America* **62,** 1116–1128.

HOWE, M. S. 1997 Edge, cavity and aperture tones at very low Mach numbers. *Journal of Fluid Mechanics* **330,** 61–84.

HOWE, M. S., SCOTT, M. I. & SIPCIC, S. R. 1996 The influence of tangential mean flow on the Rayleigh conductivity of an aperture. *Proceedings of the Royal Society of London* A**452,** 2303–2317.

KOMERATH, N. M., AHUJA, K. K. & CHAMBERS, F. W. 1987 Prediction and measurement of flows over cavities—a survey. American Institute of Aeronautics and Astronautics Paper 87–022.

KRIESELS, P. C., PETERS, M. C. A. M., HIRSCHBERG, A., WIJNANDS, A. P. J., IAFRATI, A., RICCARDI, G., PIVA, R. & BRUGGEMAN, J. C. 1995 High amplitude vortex induced pulsations in gas transport systems. *Journal of Sound and Vibration* **184,** 343–368.

LAMB, H. 1932 *Hydrodynamics;* 6th. ed., reprinted 1994. Cambridge: Cambridge University Press.

MAUNG, P. & HOWE, M. S. 1997 Vibration damping of jet nozzle flaps by vorticity production. American Institute of Aeronautics and Astronautics Paper 97–0576.

PETERS, M. C. A. M. 1993 Aeroacoustic sources in internal flows. Ph.D. Thesis, Eindhoven University of Technology, Eindhoven, The Netherlands.

POWELL, A. 1961 On the edgetone. *Journal of the Acoustical Society of America* **33,** 395–409.

RAYLEIGH, LORD 1945 *Theory of Sound,* Vol 2. New York: Dover.

ROCKWELL, D. 1983 Oscillations of impinging shear layers. *American Institute of Aeronautics and Astronautics Journal* **21,** 645–664.

ROSSITER, J. E. 1962 The effect of cavities on the buffeting of aircraft. Royal Aircraft Establishment Technical Memorandum 754.

SCOTT, M. I. 1995 The Rayleigh conductivity of a circular aperture in the presence of a grazing flow. Master's thesis, Boston University, Boston, MA, U.S.A.

TAM, C. K. W. & BLOCK, P. J. W. 1978 On the tones and pressure oscillations induced by flow over rectangular cavities. *Journal of Fluid Mechanics* **89,** 373–399.